Scientia Iranica B (2013) 20 (1), 185–194

SCIENTIA IRANICA

Sharif University of Technology

**Scientia Iranica**

*Transactions B: Mechanical Engineering*

www.sciencedirect.com

Research note

# Axisymmetric stagnation-point flow and heat transfer of a viscous, compressible fluid on a cylinder with constant heat flux

**H. Mohammadiun, A.B. Rahimi*, A. Kianifar**

*Faculty of Engineering, Ferdowsi University of Mashhad, Mashhad, P.O. Box No. 91775-1111, Iran*

Received 5 January 2012; revised 24 October 2012; accepted 10 December 2012

**KEYWORDS**

Stagnation flow;
Viscous compressible fluid;
Heat transfer;
Stationary cylinder;
Constant wall heat flux;
Exact solution.

**Abstract** Existing solutions of the problem of axisymmetric stagnation-point flow and heat transfer on either a cylinder or flat plate are for incompressible fluid. Here, fluid with temperature dependent density is considered in the problem of axisymmetric stagnation-point flow and heat transfer on a cylinder with constant heat flux. The impinging free stream is steady and with a constant strain rate, $\bar{k}$. An exact solution of the Navier–Stokes equations and energy equation is derived in this problem. A reduction of these equations is obtained by use of appropriate transformations introduced for the first time. The general self-similar solution is obtained when the wall heat flux of the cylinder is constant. All the solutions above are presented for Reynolds numbers, $Re = \bar{k}a^2/2\upsilon$, ranging from 0.01 to 1000, selected values of compressibility factors, and different values of Prandtl number, where $a$ is cylinder radius and $\nu$ is the kinematic viscosity of the fluid. For all Reynolds numbers and surface heat flux, as the compressibility factor increases, both components of the velocity field, the heat transfer coefficient and the shear-stresses increase, and the pressure function decreases.



## 1. Introduction

The study of impinging jet problems has been of considerable interest during past decades because of great technical importance in many industrial applications, such as the drying of papers and films, the tempering of glass and metal during processing, the cooling of gas turbine surfaces and electronic components, surface painting, pest-citing, and de-icing. Existing solutions of the problem of axisymmetric stagnation-point flow and heat transfer on either a cylinder or a flat plate are for viscous, incompressible fluid. These studies were started by Stokes [1] and Hiemenz [2], were continued by Von Karman [3], Griffith and Meredith [4], Homann [5], Howarth [6], Davey [7], Stuart [8–10], Kelly [11] and Wang [12,13], and further continued by Glauert [14] and Gorla [15–19], Cunning et al. [20], Weidman and Mahalingam [21], Grosch and Salwen [22] and Takhar et al. [23]. The most recent work of the same type is by Saleh and Rahimi [24], Rahimi and Saleh [25,26], and Shokrgozar and Rahimi [27–30]. Some existing compressible flow studies, but in the stagnation region of bodies and using boundary layer equations, are by Subhashini and Nath [31], Kumari and Nath [32,33], Katz [34], Afzal and Ahmad [35], Libby [36], Gersten et al. [37], and Mohammadiun and Rahimi [38], which is for constant surface temperature.

The problem of stagnation-point flow and heat transfer for the case of compressible fluid on a cylinder with constant heat flux has not been considered so far. In this research work, a solution to the problem of axisymmetric stagnation-point flow and heat transfer is presented for a case of compressible, viscous fluid on a stationary cylinder with constant heat flux. An exact solution of the Navier–Stokes equations and the energy equation is obtained. A self-similar solution is reached by introducing similarity variables derived for the first time. Sample distributions of shear-stress and temperature fields at Reynolds numbers ranging from 0.01 to 1000 are presented for different values of Prandtl number and fluid compressibility factor.

## 2. Problem formulation

Flow is considered in cylindrical coordinates $(r, \varphi, z)$ with corresponding velocity components $(u, v, w)$, as in Figure 1.

* Corresponding author. Tel.: +98 511 8805018; fax: +98 511 8763304.
*E-mail address:* rahimiab@yahoo.com (A.B. Rahimi).

Peer review under responsibility of Sharif University of Technology.

ELSEVIER Production and hosting by Elsevier

1026-3098 © 2013 Sharif University of Technology. Production and hosting by Elsevier B.V. Open access under CC BY-NC-ND license.
doi:10.1016/j.scient.2012.12.015

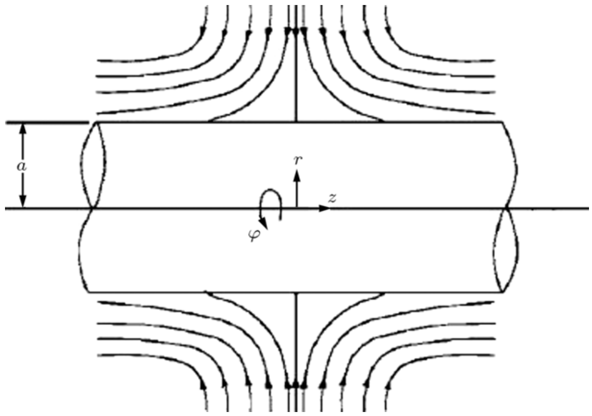


Figure 1: Schematic diagram of a stationary cylinder.

We consider the laminar steady compressible flow and heat transfer of a viscous fluid in the neighborhood of an axisymmetric stagnation-point of a stationary infinite circular cylinder with constant heat flux. An external axisymmetric radial stagnation flow of strain rate $\bar{k}$ impinges on the cylinder of radius $a$, centered at $r = 0$. The steady Navier–Stokes and energy equations in cylindrical polar coordinates governing the axisymmetric compressible flow and heat transfer are:

Mass:

$$\frac{\partial(\rho u)}{\partial r} + \frac{\rho u}{r} + \frac{\partial(\rho w)}{\partial z} = 0, \tag{1}$$

$r$-Momentum:

$$u\frac{\partial(\rho u)}{\partial r} + w\frac{\partial(\rho u)}{\partial z} = -\frac{\partial P}{\partial r} + \nu\left\{\frac{1}{r}\frac{\partial}{\partial r}\left[r\frac{\partial(\rho u)}{\partial r}\right] - \frac{(\rho u)}{r^2} + \frac{\partial^2(\rho u)}{\partial z^2}\right\}, \tag{2}$$

$z$-Momentum:

$$u\frac{\partial(\rho w)}{\partial r} + w\frac{\partial(\rho w)}{\partial z} = -\frac{\partial P}{\partial z} + \nu\left\{\frac{1}{r}\frac{\partial}{\partial r}\left[r\frac{\partial(\rho w)}{\partial r}\right] + \frac{\partial^2(\rho w)}{\partial z^2}\right\}, \tag{3}$$

$$\rho u\frac{\partial T}{\partial r} + \rho w\frac{\partial T}{\partial z} = \frac{\mu}{\mathrm{Pr}}\frac{1}{r}\frac{\partial}{\partial r}\left(r\frac{\partial T}{\partial r}\right), \tag{4}$$

where $p$, $\rho$, $\nu$, and $T$ are the fluid pressure, density, kinematic viscosity, and temperature, respectively. Boundary conditions for the velocity field are:

$$r = a: \ u = 0, \qquad w = 0, \tag{5}$$

$$r \to \infty: \ u = -\bar{k}(r - a^2/r), \qquad w = 2\bar{k}z, \tag{6}$$

in which Relation (5) are no-slip conditions on the cylinder wall and Relations (6) show that the viscous flow solution approaches, in a manner analogous to the Hiemenz flow, the potential flow solution as $r \to \infty$ [20].

For the temperature field, we have:

$$r = a: \ \frac{\partial T}{\partial r} = -\frac{q_w}{k}, \qquad r \to \infty: \ T \to T_\infty, \tag{7}$$

where, $k$ is the thermal conductivity of the fluid, $q_w$ is the heat flux at the wall cylinder, and $T_\infty$ is the free stream temperature.

A reduction of the Navier–Stokes equations is obtained by the following coordinate separation of the velocity field:

$$u = -\frac{\bar{k}a^2}{r}\frac{\rho_\infty}{\rho(\eta)}f(\eta), \qquad w = \frac{\rho_\infty}{\rho(\eta)}[2\bar{k}cf'(\eta)z], \qquad p = \rho_\infty\bar{k}^2a^2P, \tag{8}$$

where:

$$\eta = \frac{2}{a^2}\int_a^r \frac{\rho r}{\rho_\infty}dr, \tag{9}$$

is the dimensionless radial variable, the prime denotes differentiation with respect to $\eta$, and $\rho_\infty$ is free stream density. Note that, for the case of incompressible flow ($\rho(\eta) =$ constant), this variable is similar to the one in Wang [12], except that it changes from zero to infinity instead of one to infinity. Transformations in Eq. (8) satisfy Eq. (1) automatically and their insertion into Eqs. (2) and (3) yields a coupled system of differential equations in terms of $f(\eta)$, and an expression for the pressure:

$$\Gamma[c^3f''' + 3c^2c'f'' + c^2c''f' + (c')^2cf'] + c^2f'' + cc'f' + \mathrm{Re}[1 + c'ff' + cff'' - c(f')^2] = 0, \tag{10}$$

$$p - p_0 = \int_0^\eta \left[\frac{1}{2}\left(\frac{f}{\Gamma c}\right)^2 - \frac{ff'}{\Gamma c^2} - \frac{1}{\mathrm{Re}}(cf')'d\eta - 2\left(\frac{z}{a}\right)^2\right]. \tag{11}$$

In these equations;

$$c(\eta) = \frac{\rho(\eta)}{\rho_\infty}, \qquad \Gamma(\eta) = 1 + \int_0^\eta \frac{d\eta}{c(\eta)}. \tag{12}$$

$\mathrm{Re} = \frac{\bar{k}a^2}{2\nu}$ is the Reynolds number and prime indicates differentiation with respect to $\eta$. From Conditions (5) and (6), the boundary conditions for Eqs. (10) and (11) are as follows:

$$\eta = 0: \ f = 0, \qquad f' = 0, \qquad \eta \to \infty: \ f' = 1. \tag{13}$$

To model the variation of density with respect to temperature, the following Boussinesq approximation is used, assuming low Mach number flow:

$$\rho \approx \rho_\infty[1 - \beta(T - T_\infty)] \Rightarrow \rho/\rho_\infty = c(\eta) = 1 - \beta(T - T_\infty), \tag{14}$$

in which $\beta$ is the compressibility factor.

To transform the energy equation into a non-dimensional form, we introduce:

$$\theta(\eta) = \frac{T(\eta) - T_\infty}{\frac{aq_w}{2k}} = \frac{T(\eta) - T_\infty}{\gamma}. \tag{15}$$

Making use of Eqs. (8) and (15), the energy equation may be written as:

$$\frac{1}{\mathrm{Re}\cdot\mathrm{Pr}}[\Gamma(c^2\theta'' + cc'\theta') + c\theta'] + f\theta' = 0. \tag{16}$$

With boundary conditions as:

$$\eta = 0: \ -\theta'\left[1 - \beta\left(\frac{aq_w}{2k}\right)\theta\right] = 1 = -\theta'(1 - \beta\gamma\theta), \qquad \eta \to \infty: \ \theta = 0. \tag{17}$$

The local heat transfer coefficient is given by:

$$h(z) = \frac{q_w}{T_w - T_\infty} = \frac{2k}{a}\frac{1}{\theta(0)}. \tag{18}$$

Eq. (11) for a stationary cylinder is automatically satisfied and because of $c(\eta)$, Eqs. (10)–(12) and (16) are dependent. Note that, for the case of incompressible fluid, $\rho(\eta) = \rho_\infty$, Eq. (10) is exactly reduced to the equation obtained in [12] for the radial component of velocity, and also Eq. (16) reduces to the energy equation obtained in [15] with consideration of the starting value for variable $\eta$.

## 3. Shear-stress

The shear-stress on the surface of the cylinder is obtained from:

$$\sigma = \mu \left[\frac{\partial w}{\partial r}\right]_{r=a}, \tag{19}$$

where $\mu$ is the viscosity of the fluid. Using definition in Eq. (8), the shear-stress at the cylinder surface for self-similar solutions becomes:

$$\sigma = \mu[2Kf''(0)z]\frac{2}{a}C(0) \Rightarrow \frac{\sigma a}{4\mu Kz} = f''(0)C(0). \tag{20}$$

Results for $\frac{\sigma a}{4\mu Kz}$ for different values of Re, with Pr held constant, and for different values of Pr, with Re held constant, are presented in later sections.

## 4. Presentation of results

In this section, the solution of self-similar Eqs. (10) and (16), along with surface shear-stresses, for prescribed values of surface heat flux for selected values of Reynolds and Prandtl number, is presented.

Sample profiles of the $f(\eta)$ function against $\eta$ for a compressibility factor of $\beta = 0.0033$, Pr $= 0.7$, constant wall heat flux $\gamma = 30$, and for selected values of Reynolds number are presented in Figure 2. As Reynolds number increases, the depth of diffusion of the fluid velocity field in a radial direction increases. Effects of variation of compressibility factor on $f(\eta)$ function against $\eta$ for $\gamma = 10$, Pr $= 0.7$ and selected values of Reynolds number are shown in Figures 3–5. For $\beta = 0$, incompressible fluid, the results of Gorla [15] are extracted and it is interesting to note that, as $\beta$ increases, the depth of diffusion of the fluid velocity field in a radial direction increases. So, for all the Reynolds numbers, the incompressible fluid case produces the lowest value of radial velocity and, as compressibility increases, this quantity increases accordingly. The effect of the surface heat flux of the cylinder on the depth of diffusion of the fluid velocity field in a radial direction has been depicted in Figures 6–8, for $\beta = 0.0033$, Pr $= 0.7$ and selected values of Reynolds numbers. Note that, as the surface heat flux of the cylinder increases, this quantity increases for all values of Reynolds number. This is expected, since the increase of the surface heat flux and compressibility of the fluid have parallel effects.

Sample profiles of the $f'(\eta)$ function against $\eta$, for compressibility factor of $\beta = 0.0033$, Pr $= 0.7$, constant wall heat flux $\gamma = 1$ and for selected values of Reynolds number are shown in Figure 9. Again, as Reynolds number increases, the depth of diffusion of the fluid velocity field in the $z$-direction increases. Effects of variations in the compressibility factor on the $f'(\eta)$ function against $\eta$, for $\gamma = 1$, Pr $= 0.7$ and Reynolds number Re $= 1$, are shown in Figure 10. For, $\beta = 0$, incompressible fluid, the result of Gorla [15] is extracted, and it is interesting to note that as $\beta$ increases, the depth of diffusion of the fluid

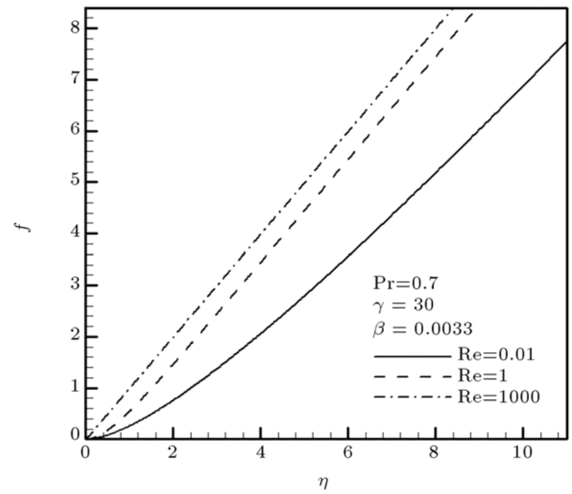


Figure 2: Variation of $f$ in terms of $\eta$ at $\gamma = 30$, $\beta = 0.0033$ and Pr $= 0.7$ for different values of Reynolds number.

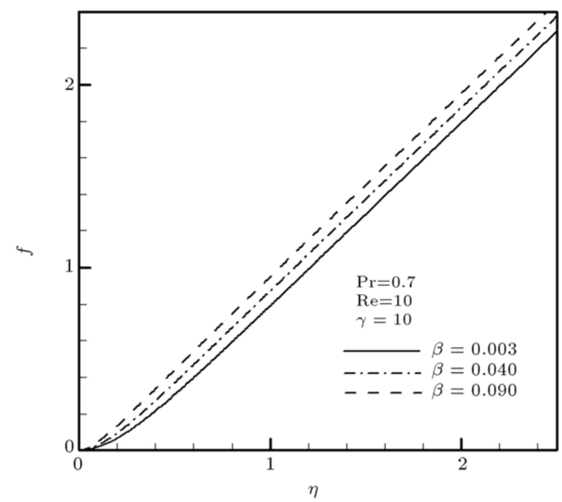


Figure 3: Variation of $f$ in terms of $\eta$ at $\gamma = 10$, Re $= 10.0$ and Pr $= 0.7$ for different values of compressibility factor.

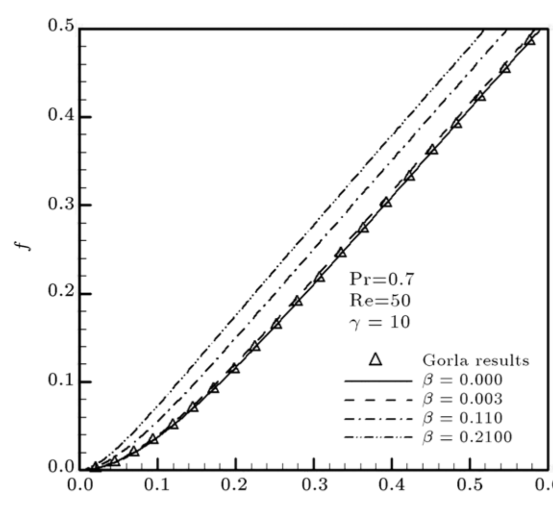


Figure 4: Variation of $f$ in terms of $\eta$ at $\gamma = 10$, Re $= 50.0$ and Pr $= 0.7$ for different values of compressibility factor.

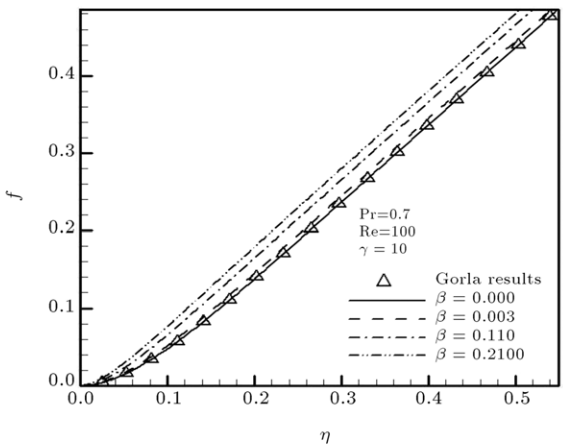


Figure 5: Variation of $f$ in terms of $\eta$ at $\gamma = 10$, Re $= 100.0$ and Pr $= 0.7$ for different values of compressibility factor.

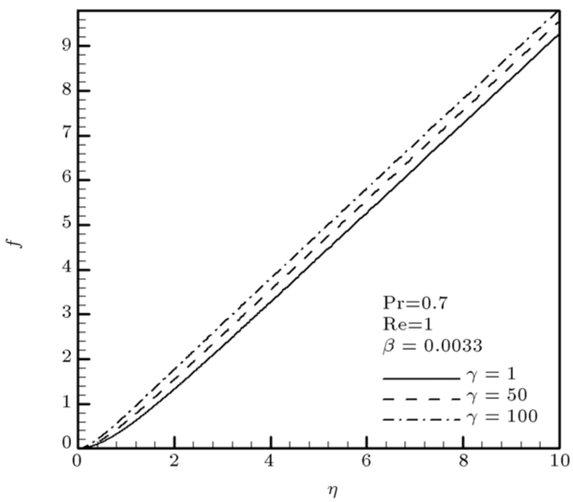


Figure 6: Variation of $f$ in terms of $\eta$ at Re $= 1.0$ and Pr $= 0.7$ for different values of wall heat flux.

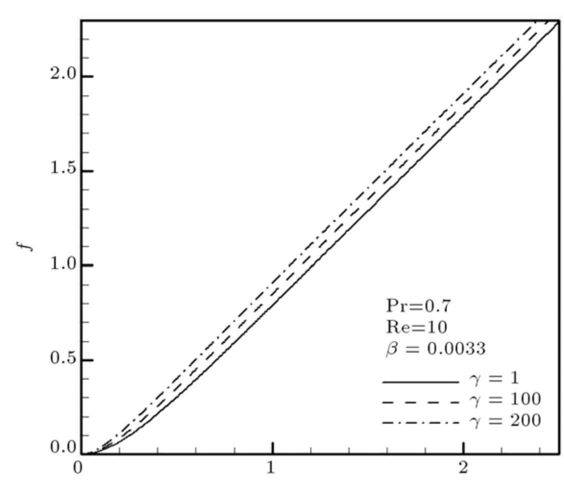


Figure 7: Variation of $f$ in terms of $\eta$ at Re $= 10.0$ and Pr $= 0.7$ for different values of wall heat flux.

velocity field in the $z$-direction also increases. Again, the incompressible fluid case produces the lowest value of velocity in the $z$-direction and, as the compressibility factor increases,

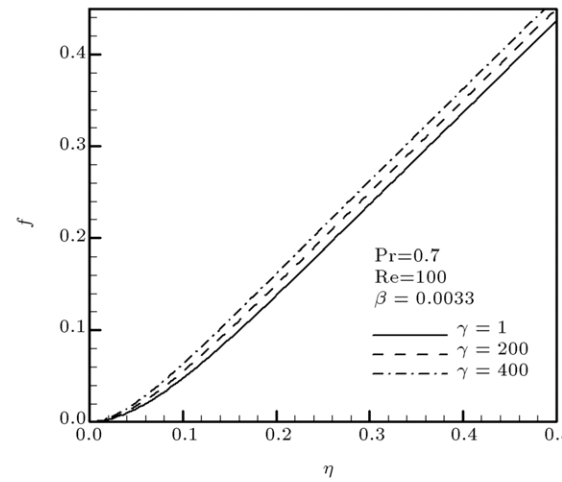


Figure 8: Variation of $f$ in terms of $\eta$ at Re $= 100.0$ and Pr $= 0.7$ for different values of wall heat flux.

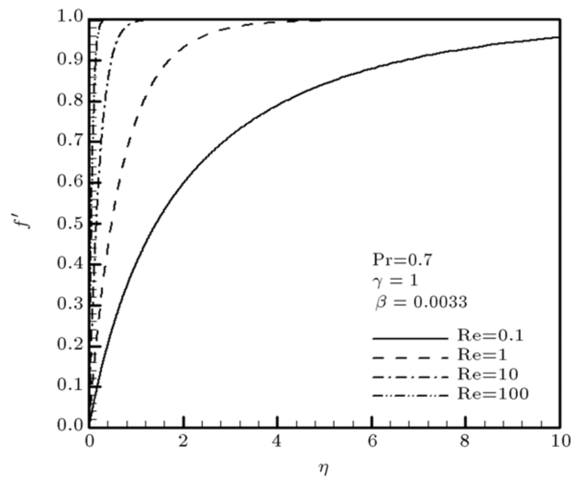


Figure 9: Variation of $f'$ in terms of $\eta$ at $\gamma = 1$, Pr $= 0.7$ and $\beta = 0.0033$ for different values of Reynolds number.

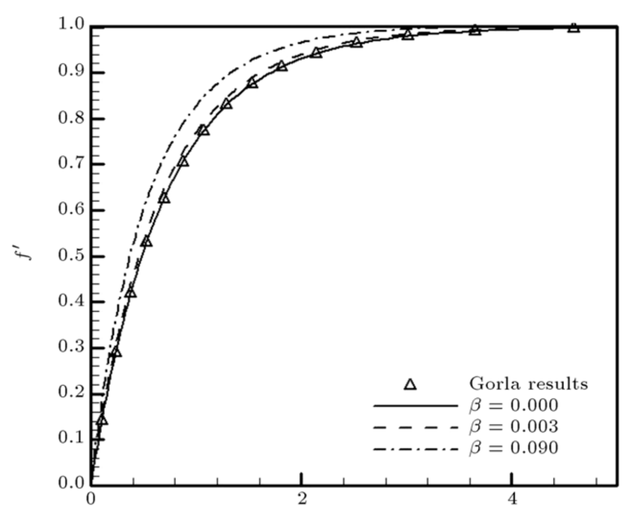


Figure 10: Variation of $f'$ in terms of $\eta$ at $\gamma = 1$, Re $= 1.0$ and Pr $= 0.7$, for different values of compressibility factor.

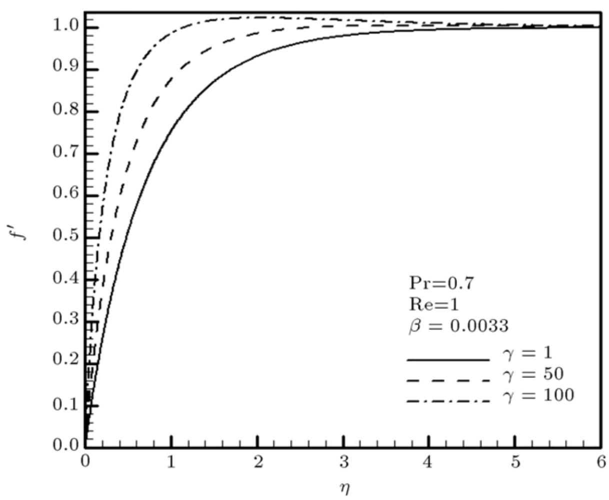


Figure 11: Variation of $f'$ in terms of $\eta$ at Re $= 1.0$, Pr $= 0.7$ and $\beta = 0.0033$ for different values of wall heat flux.

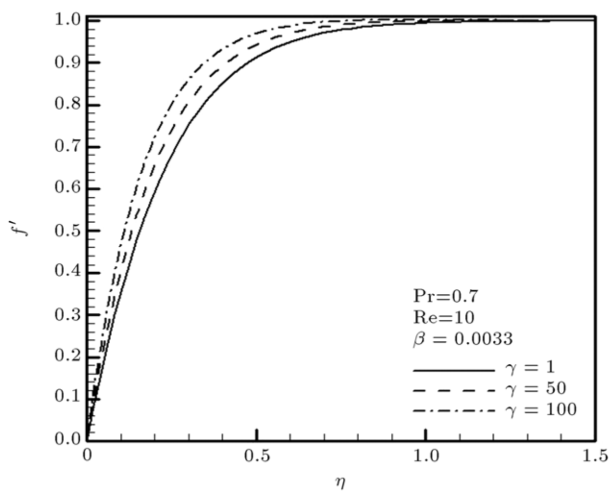


Figure 12: Variation of $f'$ in terms of $\eta$ at Re $= 1.0$, Pr $= 0.7$ and $\beta = 0.0033$ for different values of wall heat flux.

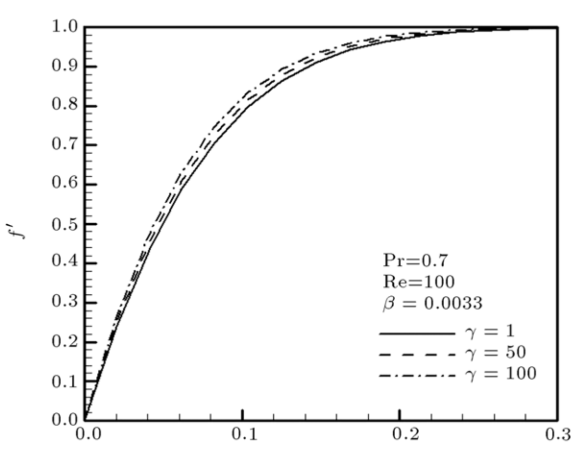


Figure 13: Variation of $f'$ in terms of $\eta$ at Re $= 100.0$, Pr $= 0.7$ and $\beta = 0.0033$ for different values of wall heat flux.

this quantity increases accordingly. Effects of the surface heat flux of the cylinder on the depth of diffusion of the fluid velocity

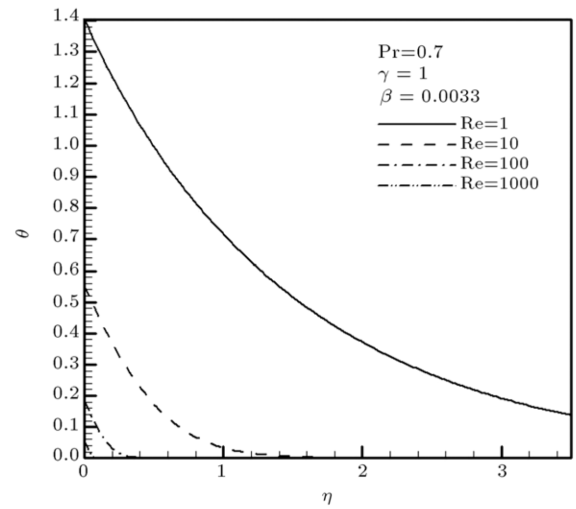


Figure 14: Variation of $\theta$ in terms of $\eta$ at $\gamma = 1$, Pr $= 0.7$ and $\beta = 0.0033$ for different values of Reynolds numbers.

field in the $z$-direction have been presented in Figures 11–13 for $\beta = 0.0033$, Pr $= 0.7$ and selected values of Reynolds number. Again, as the surface temperature of the cylinder increases, this quantity increases for all values of Reynolds number and proves that the effect of surface temperature and compressibility of fluid are in parallel for the velocity field.

Sample profiles of the $\theta(\eta)$ function against $\eta$ in the case of constant surface heat flux, for compressibility factor $\beta = 0.0033$, Pr $= 0.7$, $\gamma = 1$ and for selected values of Reynolds number, are depicted in Figure 14. As Reynolds number increases, the depth of diffusion of the thermal boundary layer decreases and, in fact, as in Eq. (18), the coefficient of heat transfer increases. Effects of variations of compressibility factor on the $\theta(\eta)$ function against $\eta$ for $\gamma = 10$, Pr $= 0.7$ and selected values of Reynolds number, are presented in Figures 15–17. For $\beta = 0$, incompressible fluid, the result of Gorla [15] is extracted and it is interesting to note that, as $\beta$ increases, the depth of diffusion of the thermal boundary layer decreases. Again, the incompressible fluid case produces the lowest value of heat transfer coefficient and, as compressibility increases, this quantity increases accordingly. The effect of variation of constant Prandtl number on the $\theta(\eta)$ function for the case of constant surface heat flux, for compressibility factor $\beta = 0.0033$, Re $= 10$, and $\gamma = 10$, is shown in Figure 18. As Prandtl number increases, the depth of diffusion of the thermal boundary layer decreases and, therefore, the heat transfer coefficient increases.

Sample profiles of pressure function against $\eta$ for the case of Pr $= 0.7$, $\gamma = 10$, $\beta = 0.0033$, and for selected values of Reynolds number are shown in Figure 19. As expected, by an increase in Reynolds number, the depth of diffusion of the fluid pressure increases. Figure 20 represents pressure for the case of Pr $= 0.7$, Re $= 10$, $\beta = 0.0033$, and different values of cylinder wall heat flux. As wall heat flux increases, pressure decreases. The effect of the compressibility factor for the case of Pr $= 0.7$, Re $= 1$, and $\gamma = 100$ is presented in Figure 21. The largest amount of pressure is produced for the case of an incompressible fluid. The effect of increase in Prandtl number on the pressure function is depicted in Figure 22, for the case of $\gamma = 100$, Re $= 10$, and $\beta = 0.0033$. As Prandtl number increases, the pressure function increases as well.

Sample profiles of surface shear-stress against cylinder wall heat flux are shown in Figure 23, for the case of Pr $= 0.7$,

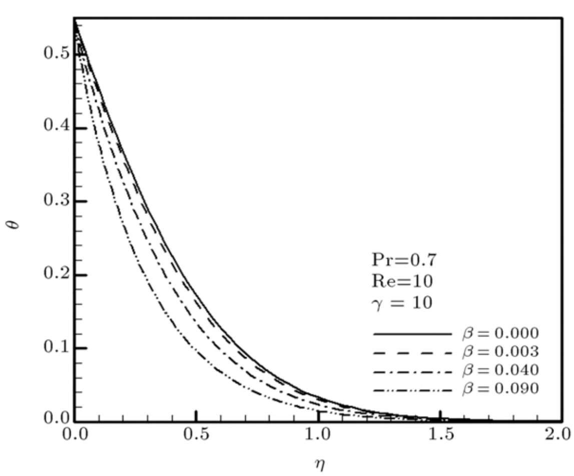


Figure 15: Variation of $\theta$ in terms of $\eta$ at $\gamma = 10.0$, $\Pr = 0.7$ and $\mathrm{Re} = 10$ for different values of compressibility factor.

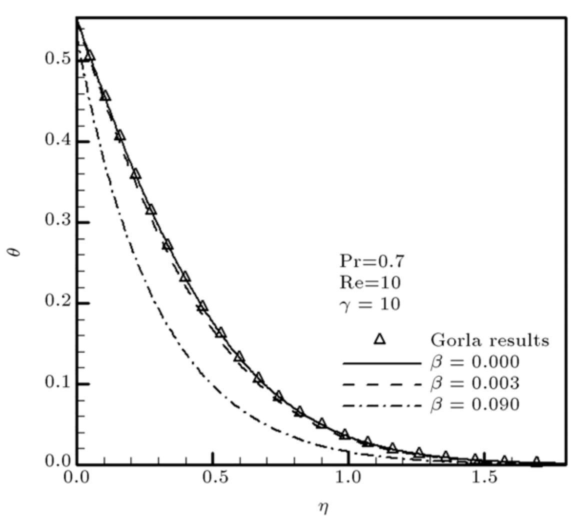


Figure 16: Variation of $\theta$ in terms of $\eta$ at $\gamma = 10.0$, $\Pr = 0.7$ and $\mathrm{Re} = 10$ for different values of compressibility factor.

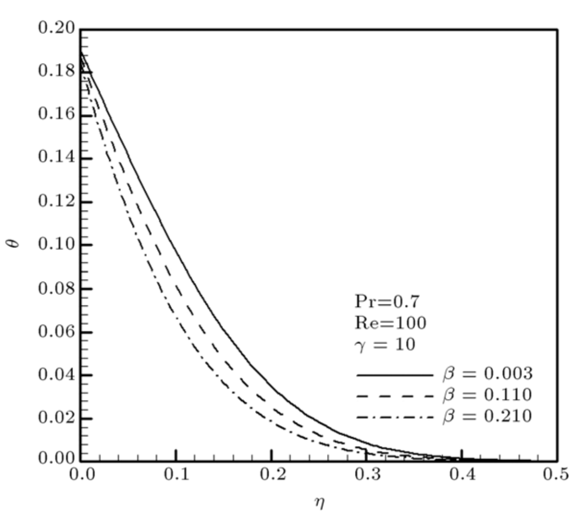


Figure 17: Variation of $\theta$ in terms of $\eta$ at $\gamma = 10.0$, $\Pr = 0.7$ and $\mathrm{Re} = 100$ for different values of compressibility factor.

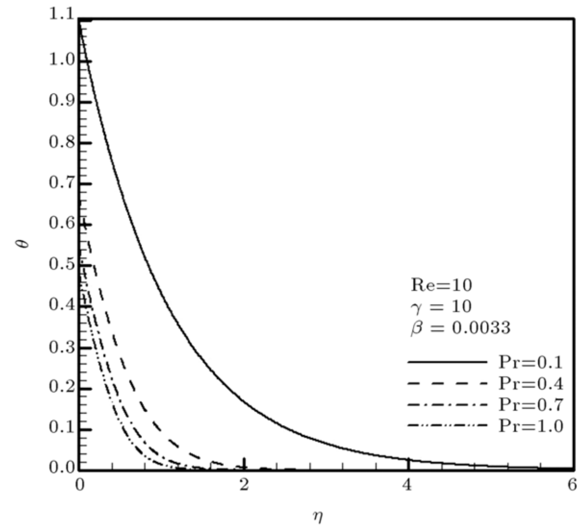


Figure 18: Variation of $\theta$ in terms of $\eta$ at $\beta = 0.0033$ and $\mathrm{Re} = 10$ for different values of Prandtl number.

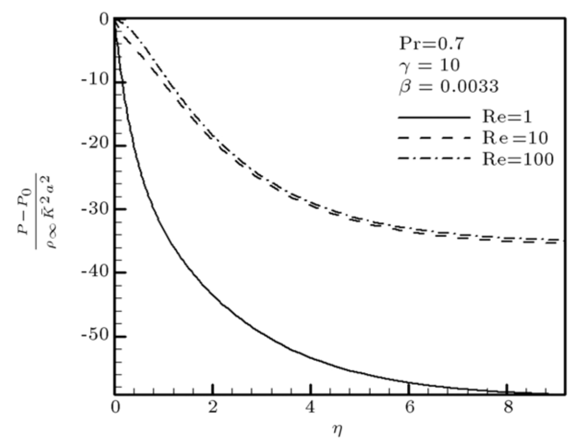


Figure 19: Variation of pressure functions in terms of $\eta$ at $\beta = 0.0033$, $\gamma = 10.0$ and $\Pr = 0.7$ for different values of Reynolds number.

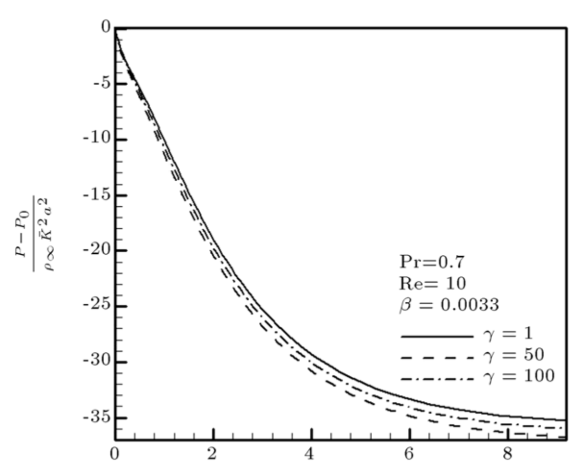


Figure 20: Variation of pressure function in terms of $\eta$ at $\mathrm{Re} = 10.0$, $\Pr = 0.7$ and $\beta = 0.0033$ for different values of wall heat flux.

$\beta = 0.0033$ and for selected values of Reynolds number. As expected, the more the Reynolds number is, the more the surface shear-stress is, and in cases of individual Reynolds number,

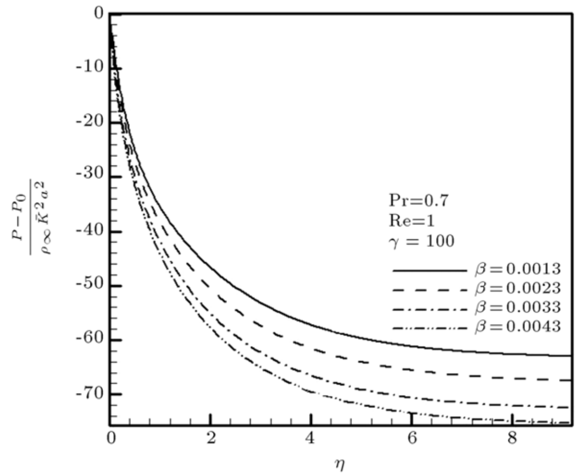


Figure 21: Variation of pressure function in terms of $\eta$ at Re $= 1.0$, Pr $= 0.7$ and $\gamma = 100$ for different values of compressibility factor.

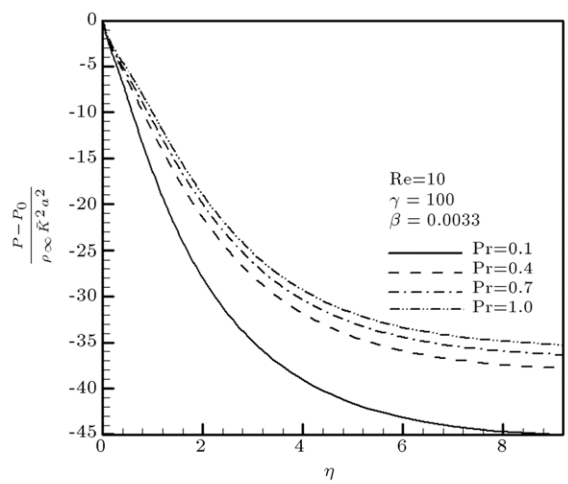


Figure 22: Variation of pressure function in terms of $\eta$ at Re $= 10.0$, $\beta = 0.0033$ and $\gamma = 100$ for different values of Prandtl number.

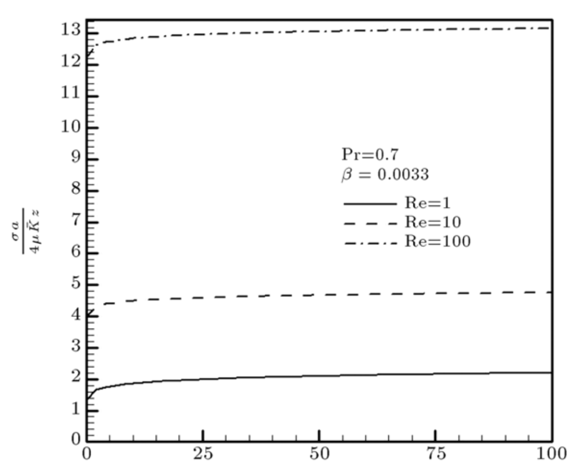


Figure 23: Variation of shear-stress in terms of $\eta$ at $\beta = 0.0033$ and Pr $= 0.7$ for different values of Reynolds number.

the value of surface shear-stress increases with surface temperature. The same information above can be concluded from

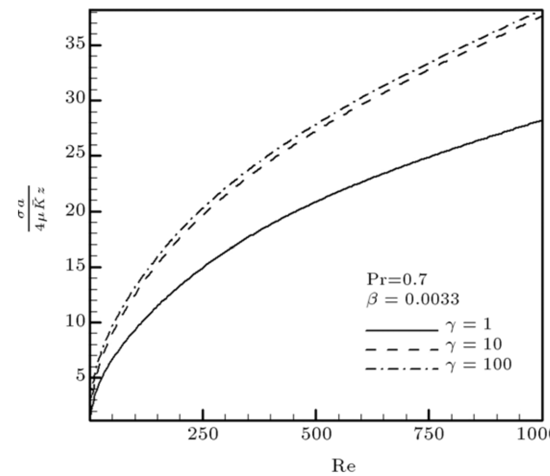


Figure 24: Variation of shear-stress in terms of Re at $\beta = 0.0033$ and Pr $= 0.7$ for different values of wall heat flux.

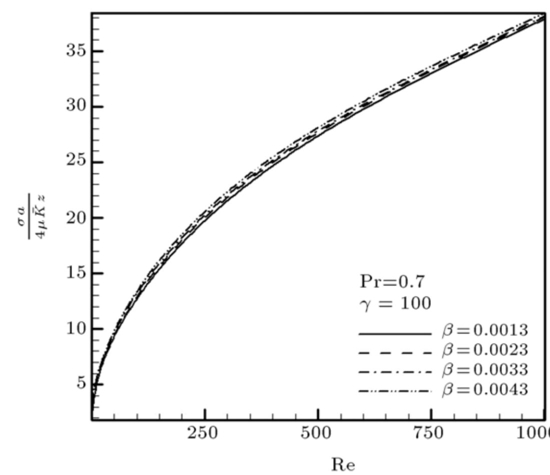


Figure 25: Variation of shear-stress in terms of Re at Pr $= 0.7$ and $\gamma = 100$ for different values of compressibility factor.

Figure 24. The effect of compressibility factor on shear-stress against Reynolds number is shown in Figure 25, for the case of Pr $= 0.7$, $\gamma = 100$. It is interesting to note that the incompressible fluid case produces the least amount of shear-stress.

## 5. Conclusions

An exact solution of the Navier–Stokes equations and energy equation has been obtained for the problem of axisymmetric stagnation-point flow on a stationary circular cylinder with constant wall heat flux. A reduction of these equations has been obtained by use of appropriate transformations introduced for the first time. The general self-similar solution has been obtained when the wall heat flux of the cylinder is constant. All the solutions above have been presented for Reynolds numbers, Re $= \bar{k}a^2/2\nu$, ranging from 0.01 to 1000, and different values of Prandtl number and compressibility factor. For all values of Reynolds number and cylinder wall heat flux, as the compressibility factor increases, the value of both components of the velocity field, heat transfer coefficient, and shear-stresses increase, and the pressure function decreases. For the case of incompressible fluid, $\rho(\eta) = \rho_\infty$ or $c(\eta) = 1$, and similarity variables and radial component of velocity by Wang [12], and energy equation by Gorla [15], are obtained.

**Acknowledgment**

This research work has been supported financially by Ferdowsi University of Mashhad, based on contract number 2/19730.

**Appendix**

Details of derivation of Eqs. (10), (11) and (16) are presented below:

$$\eta = \frac{2}{a^2}\int_a^r \frac{\rho r}{\rho_\infty}dr \Rightarrow \frac{d\eta}{dr} = \frac{2\rho r}{a^2\rho_\infty} \rightarrow \frac{d\eta}{dr}$$
$$= \frac{2r}{a^2}c(\eta) \rightarrow 2rdr = a^2\frac{d\eta}{c(\eta)} \xrightarrow{\int} \int_a^r 2rdr$$
$$= a^2\int_0^\eta \frac{d\eta}{c(\eta)} \rightarrow r^2 - a^2 = a^2\int_0^\eta \frac{d\eta}{c(\eta)} \rightarrow r^2$$
$$= a^2\left[1+\int_0^\eta \frac{d\eta}{c(\eta)}\right].$$

With definition $\Gamma(\eta) = [1+\int_0^\eta \frac{d\eta}{c(\eta)}]$ we have:

$$r^2 = a^2\Gamma(\eta).$$

(1) To derive pressure:

By use of non-dimensional pressure as:

$$p = \frac{P}{\rho_\infty K^2 a^2} \Rightarrow P = \rho_\infty K^2 a^2 p.$$

Start from $r$-momentum:

$$u\frac{\partial(\rho u)}{\partial r} + w\frac{\partial(\rho u)}{\partial z}$$
$$= -\frac{\partial P}{\partial r} + \nu\left\{\frac{1}{r}\frac{\partial}{\partial r}\left[r\frac{\partial(\rho u)}{\partial r}\right] - \frac{(\rho u)}{r^2} + \frac{\partial^2(\rho u)}{\partial z^2}\right\}.$$

But:

$$\rho u = -\frac{Ka^2}{r}\rho_\infty f(\eta) \Rightarrow \frac{\partial(\rho u)}{\partial r} = \frac{Ka^2}{r^2}\rho_\infty f - 2K\rho_\infty cf'$$
$$\Rightarrow r\frac{\partial(\rho u)}{\partial r} = \frac{Ka^2}{r}\rho_\infty f - 2K\rho_\infty cf' r$$
$$\Rightarrow \frac{\partial}{\partial r}\left[r\frac{\partial(\rho u)}{\partial r}\right] = -\frac{Ka^2}{r^2}\rho_\infty f + \frac{Ka^2}{r}\rho_\infty f'(\eta)\frac{2r}{a^2}c$$
$$-2K\rho_\infty(cf')'\frac{2r^2}{a^2}c - 2K\rho_\infty cf' \Rightarrow \frac{1}{r}\frac{\partial}{\partial r}\left[r\frac{\partial(\rho u)}{\partial r}\right]$$
$$= -\frac{Ka^2}{r^3}\rho_\infty f - \frac{4Kr}{a^2}\rho_\infty c(cf')'.$$

Then, $r$-momentum is:

$$-\frac{Ka^2}{r}\frac{\rho_\infty}{\rho}f(\eta)\left[\frac{Ka^2}{r^2}\rho_\infty f(\eta) - 2K\rho_\infty cf'\right]$$
$$= -\rho_\infty K^2a^2\frac{\partial p}{\partial \eta}\frac{2r}{a^2}c + \nu\left[-\frac{Ka^2}{r^3}\rho_\infty f\right.$$
$$\left. - \frac{4Kr}{a^2}\rho_\infty c(cf')' + \frac{Ka^2}{r^3}\rho_\infty f\right].$$

After omitting underlined phrases:

$$-\frac{K^2a^4}{r^3}\frac{\rho_\infty}{\rho}\rho_\infty f^2 + \frac{2K^2a^2}{r}\frac{\rho_\infty}{\rho}\rho_\infty ff'$$
$$= -2\rho_\infty K^2cr\frac{\partial p}{\partial \eta} - \frac{4K\nu}{a^2}rc\rho_\infty(cf')'.$$

Dividing by $2K^2r\rho_\infty$ and using $r^2 = a^2\Gamma(\eta)$;

$$-\frac{1}{2}\frac{a^4}{r^4}\frac{f^2}{c} + \frac{a^2}{r^2}\frac{ff'}{c} = -c\frac{\partial p}{\partial \eta} - \frac{2\nu}{Ka^2}c(cf')' \xrightarrow{r^2=a^2\phi(\eta)} \frac{\partial p}{\partial \eta}$$
$$= \frac{1}{2}\left(\frac{f}{\Gamma c}\right)^2 - \frac{ff'}{\Gamma c^2} - \frac{1}{\mathrm{Re}}(cf')'.$$

Integrating this, we have:

$$p - p_0 = \int_0^\eta\left[\frac{1}{2}\left(\frac{f}{\Gamma c}\right)^2 - \frac{ff'}{\Gamma c^2} - \frac{1}{\mathrm{Re}}(cf')'\right]d\eta + c_1(Z).$$

Here, $c_1$ is a function of $z$ which will be calculated by use of $z$-momentum as:

$$u\frac{\partial(\rho w)}{\partial r} + w\frac{\partial(\rho w)}{\partial z} = -\frac{\partial P}{\partial z}.$$

But, at $r \rightarrow \infty$ : $\rho w = 2Kz\rho_\infty \Rightarrow \begin{cases}\frac{\partial(\rho w)}{\partial r} = 0\\ \frac{\partial(\rho w)}{\partial z} = 2K\rho_\infty\end{cases}$, $\frac{\partial P}{\partial z} = \rho_\infty K^2a^2\frac{\partial p}{\partial z}$.

Then:

$$-\rho_\infty K^2a^2\frac{dc_1(z)}{dz} = 2Kz(2K\rho_\infty) \Rightarrow \frac{dc_1(z)}{dz} = -\frac{4z}{a^2} \Rightarrow c_1(z)$$
$$= -2\left(\frac{z}{a}\right)^2,$$

which gives the pressure as:

$$p - p_0 = \int_0^\eta\left[\frac{1}{2}\left(\frac{f}{\Gamma c}\right)^2 - \frac{ff'}{\Gamma c^2} - \frac{1}{\mathrm{Re}}(cf')'\right]d\eta - 2\left(\frac{z}{a}\right)^2.$$

(2) To derive Eqs. (10) and (11):

Start from $z$-momentum:

$$u\frac{\partial(\rho w)}{\partial r} + w\frac{\partial(\rho w)}{\partial z}$$
$$= -\frac{\partial P}{\partial z} + \nu\left\{\frac{1}{r}\frac{\partial}{\partial r}\left[r\frac{\partial(\rho w)}{\partial r}\right] + \frac{\partial^2(\rho w)}{\partial z^2}\right\}.$$

But:

$$\frac{\partial(\rho w)}{\partial r} = \frac{\partial(\rho w)}{\partial \eta}\frac{\partial \eta}{\partial r}$$
$$= (2Kc'f'z + 2Kcf''z)\rho_\infty\frac{2r}{a^2}c \Rightarrow r\frac{\partial(\rho w)}{\partial r}$$
$$= (2Kcc'f'z + 2Kc^2f''z)\rho_\infty\frac{2r^2}{a^2} \Rightarrow \frac{\partial}{\partial r}\left[r\frac{\partial(\rho w)}{\partial r}\right]$$
$$= [2Kcc'f'z + 2Kc^2f''z]\rho_\infty\frac{4r}{a^2}$$
$$+ [2K(c')^2cf'z + 2Kc^2c''f'z + 6Kc^2c'f''z$$
$$+ 2Kc^3f'''z]\rho_\infty\frac{4r^3}{a^4} \Rightarrow \frac{1}{r}\frac{\partial}{\partial r}\left[r\frac{\partial(\rho w)}{\partial r}\right]$$
$$= [2Kcc'f'z + 2Kc^2f''z]\rho_\infty\frac{4}{a^2} + [2K(c')^2cf'z$$
$$+ 2Kc^2c''f'z + 6Kc^2c'f''z + 2Kc^3f'''z]\rho_\infty\frac{4}{a^2}\Gamma(\eta).$$

Substitute in $z$-momentum:

$$-\frac{Ka^2}{r}\frac{\rho_\infty}{\rho}f(2Kc'f'z+2Kcf''z)\rho_\infty\frac{2r}{a^2}\frac{\rho}{\rho_\infty}+\frac{1}{\rho}(2K\rho_\infty cf'z)2K\rho_\infty\frac{\rho}{\rho_\infty}f'$$
$$=\nu\left\{[2Kcc'fz+2Kc^2f''z]\rho_\infty\frac{4}{a^2}+[2K(c')^2cf'z+2Kc^2c''f'z+6Kc^2c'f''z+2Kc^3f'''z]\rho_\infty\frac{4}{a^2}\Gamma(\eta)\right\}$$
$$-\rho_\infty K^2a^2\left(-\frac{4z}{a^2}\right).$$

Equating the coefficient of $z$, the equation for $f$ is:

$$-4K^2c'ff'-4K^2cff''+4K^2c(f')^2=\frac{8K\nu}{a^2}cc'f'+\frac{8K\nu}{a^2}c^2f''+\frac{8K\nu}{a^2}(c')^2c\Gamma f'+\frac{8K\nu}{a^2}c^2c''\Gamma f'+\frac{24K\nu}{a^2}c^2c'f''+\frac{8K\nu}{a^2}c^3\Gamma f'''+4K^2.$$

(3) To derive the energy equation, Eq. (16):

Consider a change of variable as $T(\eta)/T_\infty=g(\eta)$. Then, the energy equation can be written as:

$$\rho u\frac{\partial g}{\partial r}+\rho w\frac{\partial g}{\partial z}=\frac{\mu}{\Pr}\frac{1}{r}\frac{\partial}{\partial r}\left(r\frac{\partial g}{\partial r}\right).$$

Using the chain rule:

$$\frac{\partial g}{\partial r}=\frac{\partial g}{\partial \eta}\frac{\partial \eta}{\partial r}=\frac{2r}{a^2}cg',\qquad \frac{\partial g}{\partial z}=0.$$

$$r\frac{\partial g}{\partial r}=\frac{2r^2}{a^2}cg'\Rightarrow\frac{\partial}{\partial r}\left(r\frac{\partial g}{\partial r}\right)=\frac{4r}{a^2}cg'+\left(c'g'+cg''\right)\frac{4r^3}{a^4}c$$
$$\Rightarrow\frac{1}{r}\left[\frac{\partial}{\partial r}\left(r\frac{\partial g}{\partial r}\right)\right]=\frac{4}{a^2}cg'+\left(c'g'+cg''\right)\frac{4r^2}{a^4}c$$
$$\xrightarrow{r^2=a^2\Gamma(\eta)}\frac{1}{r}\left[\frac{\partial}{\partial r}\left(r\frac{\partial g}{\partial r}\right)\right]=\frac{4}{a^2}cg'+\frac{4\Gamma}{a^2}c\left(c'g'+cg''\right).$$

By substitution:

$$-\frac{Ka^2}{r}\rho_\infty f\frac{2r}{a^2}\frac{\rho}{\rho_\infty}g'=\frac{\mu}{\Pr}\frac{4}{a^2}(cg'+\Gamma cc'g'+\Gamma c^2g'')$$

divide by $2k\rho$ and since $1/\text{Re}=2\nu/ka^2$;

$$\frac{1}{\text{Re}\cdot\Pr}(c^2\Gamma g''+\Gamma cc'g'+cg')+fg'=0.$$

## References


[1] Stokes, G.G. "On the effect of the internal friction of fluids on the motion of pendulum", *Transaction of the Cambridge Philosophical Society*, 9(Pt. 2), pp. 8–106 (1851).

[2] Hiemenz, K. "Boundary layer for movement of a steady fluid passing through a cylinder", *Dinglers Polytechnic Journal*, 326, pp. 321–410 (1911).

[3] Von Karman, T. "About laminar and turbulence friction", *Zeitschrift für Angewandte Mathematik und Mechanik*, 1, pp. 233–252 (1921).

[4] Griffith, A.A. and Meredith, F.W. "The possible improvement in aircraft performance due to the use of boundary layer suction", Report No. E. 3501, Royal Aircraft Establishment, p. 12 (1936).

[5] Homann, F.Z. "The greatest effect of vortex stream on the surface of a cylinder and a sphere", *Journal of Mathematics and Mechanics*, 16, pp. 153–164 (1936).

[6] Howarth, L. "The boundary layer in three-dimensional flow. Part II. The flow near stagnation point", *Philosophical Magazine*, 42, pp. 1433–1440 (1951).

[7] Davey, A. "Boundary layer flow at a saddle point of attachment", *Journal of Fluid Mechanics*, 10, pp. 593–610 (1951).

[8] Stuart, J.T. "On the effects of uniform suction on the steady flow due to a rotating disk", *Quarterly Journal of Mechanics and Applied Mathematics*, 7(4), pp. 446–457 (1954).

[9] Stuart, J.T. "A solution of the Navier–Stokes and energy equations illustrating the response of skin friction and temperature of an infinite plate thermometer to fluctuations in the stream velocity", *Proceedings of The Royal Society of London. Series A*, 231(1184), pp. 116–130 (1955).

[10] Stuart, J.T. "The viscous flow near a stagnation-point when the external flow has uniform vorticity", *Journal of Aerospace Science and Technology*, 26, pp. 124–125 (1959).

[11] Kelly, R.E. "The flow of a viscous fluid past a wall of infinite extent with time-dependent suction", *Quarterly Journal of Mechanics and Applied Mathematics*, 18(3), pp. 287–298 (1965).

[12] Wang, C.Y. "Axisymmetric stagnation flow on a cylinder", *Quarterly of Applied Mathematics*, 32, pp. 207–213 (1974).

[13] Wang, C.Y. "Axisymmetric stagnation flow towards a moving plate", *American Institute of Chemical Engineers. Journal*, 19(2), pp. 1080–1082 (1973).

[14] Glauert, M.B. "The laminar boundary layer on oscillating plates and cylinders", *Journal of Fluid Mechanics*, 1, pp. 97–110 (1956).

[15] Gorla, R.S.R. "Heat transfer in an axisymmetric stagnation flow on a cylinder", *Applied Scientific Research*, 32, pp. 541–553 (1976).

[16] Gorla, R.S.R. "Unsteady laminar axisymmetric stagnation flow over a circular cylinder", *Development in Mechanics Journal*, 9, pp. 286–288 (1977).

[17] Gorla, R.S.R. "Nonsimilar axisymmetric stagnation flow on a moving cylinder", *International Journal of Science*, 16, pp. 392–400 (1978).

[18] Gorla, R.S.R. "Transient response behavior of an axisymmetric stagnation flow on a circular cylinder due to time-dependent free stream velocity", *Letters in Applied and Engineering Sciences*, 16, pp. 493–502 (1978).

[19] Gorla, R.S.R. "Unsteady viscous flow in the vicinity of an axisymmetric stagnation-point on a cylinder", *International Journal of Science*, 17, pp. 87–93 (1979).

[20] Cunning, G.M., Davis, A.M.J. and Weidman, P.D. "Radial stagnation flow on a rotating cylinder with uniform transpiration", *Journal of Engineering Mathematics*, 33, pp. 113–128 (1998).

[21] Weidman, P.D. and Mahalingam, S. "Axisymmetric stagnation-point flow impinging on a transversely oscillating plate with suction", *Journal of Engineering Mathematics*, 31, pp. 305–318 (1997).

[22] Grosch, C.E. and Salwen, H. "Oscillating stagnation-point flow", *Proceedings of The Royal Society of London. Series A*, 384, pp. 175–190 (1982).

[23] Takhar, H.S., Chamkha, A.J. and Nath, J. "Unsteady axisymmetric stagnation-point flow of a viscous fluid on a cylinder", *International Journal of Engineering Science*, 37, pp. 1943–1957 (1999).

[24] Saleh, R. and Rahimi, A.B. "Axisymmetric stagnation-point flow and heat transfer of a viscous fluid on a moving cylinder with time-dependent axial velocity and uniform transpiration", *Journal of Fluids Engineering*, 126, pp. 997–1005 (2004).

[25] Rahimi, A.B. and Saleh, R. "Axisymmetric stagnation-point flow and heat transfer of a viscous fluid on a rotating cylinder with time-dependent angular velocity and uniform transpiration", *Journal of Fluids Engineering*, 129, pp. 107–115 (2007).

[26] Rahimi, A.B. and Saleh, R. "Similarity solution of unaxisymmetric heat transfer in stagnation-point flow on a cylinder with simultaneous axial and rotational movements", *Journal of Heat Transfer, Technical Brief*, 130, pp. 054502-1–054502-5 (2008).

[27] Shokrgozar Abbasi, A. and Rahimi, A.B. "Non-axisymmetric three-dimensional stagnation-point flow and heat transfer on a flat plate", *Journal of Fluids Engineering*, 131(4), pp. 074501.1–074501.5 (2009).

[28] Shokrgozar Abbasi, A. and Rahimi, A.B. "Three-dimensional stagnation-point flow and heat transfer on a flat plate with transpiration", *Journal of Thermophysics and Heat Transfer*, 23(3), pp. 513–521 (2009).

[29] Shokrgozar Abbasi, A., Rahimi, A.B. and Niazman, H. "Exact solution of three-dimensional unsteady stagnation flow on a heated plate", *Journal of Thermodynamics and Heat Transfer*, 25(1), pp. 55–58 (2011).

[30] Shokrgozar Abbasi, A. and Rahimi, A.B. "Investigation of two-dimensional stagnation-point flow and heat transfer impinging on a flat plate", *Journal of Heat Transfer*, 134, pp. 024501-1–024501-6 (2012).

[31] Subhashini, S.V. and Nath, G. "Unsteady compressible flow in the stagnation region of two-dimensional and axisymmetric bodies", *Acta Mechanica*, 134, pp. 135–145 (1999).

[32] Kumari, M. and Nath, G. "Self-similar solution of unsteady compressible three-dimensional stagnation-point boundary layers", *Journal of Applied Mathematics and Physics*, 32, (1981).

[33] Katz, A. "Transformations of the compressible boundary layer equations", *SIAM Journal on Applied Mathematics*, 22(4), pp. 599–603 (1972).

[34] Kumari, M. and Nath, G. "Unsteady compressible 3-dimensional boundary layer flow near an axisymmetric stagnation point with mass transfer", *International Journal of Engineering Science*, 18, pp. 1285–1300 (1980).
[35] Afzal, N. and Ahmad, S. "Effect of suction and injection on self-similar solutions of second-order boundary layer equations", *International Journal of Heat and Mass Transfer*, 18, pp. 607–614 (1975).
[36] Libby, P.A. "Heat and mass transfer at a general three-dimensional stagnation point", *AIAA Journal*, 5(3), pp. 507–517 (1967).
[37] Gersten, K., Papenfuss, H.D. and Gross, J.F. "Influence of the Prandtl number on second-order heat transfer due to surface curvature at a three-dimensional stagnation point", *International Journal of Heat and Mass Transfer*, 21, pp. 275–284 (1978).
[38] Mohammadiun, H. and Rahimi, A.B. "Stagnation-point flow and heat transfer of a viscous compressible fluid on a cylinder with constant temperature", *Journal of Thermophysics and Heat Transfer*, 36(3), pp. 494–502 (2012).

**Hamid Mohammadiun** was born in Shahrood, Iran, in 1977. He received his B.S. degree in Mechanical Engineering from Amir Kabir University, Tehran, Iran in 2001 and his M.S. degree in Mechanical Engineering from Ferdowsi University of Mashhad, Iran, in 2004, where he has been a Ph.D. degree student since 2009. At present, he is Lecturer in the Department of Mechanical Engineering at the Shahrood Branch of the Islamic Azad University, Iran. His research and teaching interests include: heat transfer, fluid dynamics, applied mathematics and computational fluid dynamics (CFD).

**Asghar Baradaran Rahimi** was born in Mashhad, Iran, in 1951. He received his B.S degree in Mechanical Engineering from Tehran Polytechnic, Iran, in 1974, and a Ph.D. degree in Mechanical Engineering from the University of Akron, Ohio, USA, in 1986. He has been Professor in the Department of Mechanical Engineering at Ferdowsi University of Mashhad since 2001. His research and teaching interests include: heat transfer and fluid dynamics, gas dynamics, continuum mechanics, applied mathematics and singular perturbation.

**Ali Kianifar** was born in Mashhad, Iran, in 1955. He received his B.S. degree in Mechanical Engineering from London University in 1981, a M.S. degree in Mechanical Engineering from Bath University, UK, in 1982, and a Ph.D. degree in Mechanical Engineering from the University of Strathclyde, Glascow, UK, in 1988. He has been Associate Professor in the Department of Mechanical Engineering at Ferdowsi University of Mashhad, Iran, since 2008. His research and teaching interests include: renewable energy and fluid mechanics.